TLR2-mediated innate immune priming boosts lung anti-viral immunity

Jason Girkin[1,2,6], Su-Ling Loo[1,2,6], Camille Esneau[1,2], Steven Maltby[1,2], Francesca Mercuri[3], Brendon Chua[4], Andrew T. Reid[1,2], Punnam Chander Veerati[1,2], Chris L. Grainge[2,5], Peter A.B. Wark[2,5], Darryl Knight[2], David Jackson[4], Christophe Demaison[3] and Nathan W. Bartlett[1,2]

[1]Viral Immunology and Respiratory Disease group, University of Newcastle, Newcastle, Australia. [2]Priority Research Centre for Healthy Lungs, University of Newcastle and Hunter Medical Research Institute, Newcastle, Australia. [3]Ena Respiratory Pty Ltd, Melbourne, Australia. [4]Dept of Microbiology and Immunology, Peter Doherty Institute for Infection and Immunity, University of Melbourne, Melbourne, Australia. [5]Dept of Respiratory and Sleep Medicine, John Hunter Hospital, Newcastle, Australia. [6]These authors contributed equally.

Corresponding author: Nathan W. Bartlett (nathan.bartlett@newcastle.edu.au)

Shareable abstract (@ERSpublications)
TLR2-agonist treatment to the respiratory tract activates airway epithelial cells to prime the innate immune system to rapidly respond to infection and reduce virus-induced inflammation, including in the context of corticosteroid treatment and in asthma https://bit.ly/3g02Q4M

Cite this article as: Girkin J, Loo S-L, Esneau C, *et al*. TLR2-mediated innate immune priming boosts lung anti-viral immunity. *Eur Respir J* 2021; 58: 2001584 [DOI: 10.1183/13993003.01584-2020].

This article has supplementary material available from erj.ersjournals.com

Received: 5 May 2020
Accepted: 27 Nov 2020

Abstract

Background We assessed whether Toll-like receptor (TLR)2 activation boosts the innate immune response to rhinovirus infection, as a treatment strategy for virus-induced respiratory diseases.

Methods We employed treatment with a novel TLR2 agonist (INNA-X) prior to rhinovirus infection in mice, and INNA-X treatment in differentiated human bronchial epithelial cells derived from asthmatic-donors. We assessed viral load, immune cell recruitment, cytokines, type I and III interferon (IFN) production, as well as the lung tissue and epithelial cell immune transcriptome.

Results We show, *in vivo*, that a single INNA-X treatment induced innate immune priming characterised by low-level IFN-λ, Fas ligand, chemokine expression and airway lymphocyte recruitment. Treatment 7 days before infection significantly reduced lung viral load, increased IFN-β/λ expression and inhibited neutrophilic inflammation. Corticosteroid treatment enhanced the anti-inflammatory effects of INNA-X. Treatment 1 day before infection increased expression of 190 lung tissue immune genes. This tissue gene expression signature was absent with INNA-X treatment 7 days before infection, suggesting an alternate mechanism, potentially *via* establishment of immune cell-mediated mucosal innate immunity. *In vitro*, INNA-X treatment induced a priming response defined by upregulated IFN-λ, chemokine and anti-microbial gene expression that preceded an accelerated response to infection enriched for nuclear factor (NF)-κB-regulated genes and reduced viral loads, even in epithelial cells derived from asthmatic donors with intrinsic delayed anti-viral immune response.

Conclusion Airway epithelial cell TLR2 activation induces prolonged innate immune priming, defined by early NF-κB activation, IFN-λ expression and lymphocyte recruitment. This response enhanced anti-viral innate immunity and reduced virus-induced airway inflammation.

Introduction

Rhinoviruses (RV) are responsible for up to 60% of annual respiratory illnesses worldwide [1, 2]. Lower respiratory infections can cause cough, shortness of breath, chest tightness, wheezing, bronchiolitis and pneumonia [3]. RV is also a major cause of exacerbations of chronic respiratory diseases, including asthma [4], chronic obstructive pulmonary disease (COPD) [5, 6], cystic fibrosis (CF) [7, 8] and non-CF bronchiectasis [9]. Currently, treatments for RV infection are supportive, reducing symptoms but not limiting virus infection.

Neutrophilic inflammation constitutes the primary response to virus infection. However, excessive/prolonged neutrophilic inflammation contributes to tissue damage and increased airway neutrophil numbers correlate with exacerbation severity in asthma and COPD [10, 11]. Inhaled corticosteroids (ICS) reduce the risk of exacerbations and are a primary treatment approach for both asthma and COPD. However, ICS treatment has limited efficacy on exacerbation pathology, particularly in the context of reducing neutrophilic inflammation in asthma [12]. Further, ICS treatment suppresses anti-microbial immunity and increases susceptibility to secondary infections and pneumonia, in the context of COPD [13].

Airway epithelial cells are a primary site of rhinovirus infection. Toll-like receptors (TLRs) expressed by epithelial cells such as intracellular TLR3/7/8/9 initiate host anti-viral innate immunity, through recognition of viral nucleic acids generated by replicating virus [14]. This observation has led to the assessment of TLR agonists as anti-viral therapies. However, studies assessing viral nucleic acid-sensing TLR agonist treatment reported a narrow therapeutic window, with activation of type-I interferon (IFN) responses, inflammation, flu-like symptoms and cytokine storm [15, 16]. In contrast, TLR2 is expressed on the cell surface and is persistently exposed to both commensal microbiota and potential pathogens. As such, TLR2 activation must be tightly regulated to maintain immune homeostasis [17], which may limit unintended side effects following TLR agonist treatments. We have previously reported that TLR2 agonist treatment reduced viral load and limited transmission of influenza in mice [18], but the use of TLR2 agonists to limit other viral infections remained unexplored.

In the current study, we assessed the effects of TLR2 agonist treatment on RV infection, using the novel molecule, INNA-X. INNA-X is a pegylated analogue of the synthetic diacylated lipopeptide *S*-(2,3-bis (palmitoyl oxy)propyl) cysteine Pam2Cys [18], in which the four lysine residues traditionally used to increase solubility are replaced by polyethylene glycol. The lysine moieties were replaced as a strategy to negate off-target effects, as are observed for the closely-related TLR2 agonist, Pam3Cys [19].

Intranasal delivery of INNA-X to the lungs of mice induced innate immune priming characterised by early, low-level expression of IFN-λ and lymphocyte recruitment. Treatment 1 day before infection boosted anti-viral innate immune signatures in lung tissue and suppressed viral load. TLR2 agonist treatment 7 days before RV-A1 infection suppressed viral load and lung inflammation. Treatment efficacy persisted when consecutive doses were administered weekly. Combination treatment with inhaled corticosteroid was equally effective at reducing lung viral load and further reduced virus-induced inflammation. In differentiated primary bronchial epithelial cells (BECs) *in vitro*, INNA-X treatment also boosted innate immunity, resulting in increased early expression of IFN-λ and nuclear factor (NF)-κB-regulated antimicrobial genes. Further, IFN-λ induction preceded accelerated host anti-viral responses in differentiated primary BECs isolated from donors with asthma. This is a key finding, as multiple lines of evidence have reported inadequate anti-viral responses in asthmatics [20–22]. Our findings suggest that airway-delivered TLR2 agonist treatment of the respiratory epithelium provides sustained airway innate immune priming and is an effective strategy to limit respiratory virus infection and infection-induced airway inflammation.

Materials and methods

Ethics statements

Primary bronchial epithelial cells were provided by P.A.B. Wark (The University of Newcastle, Newcastle, Australia), obtained from healthy donors or donors with asthma during bronchoscopy, with written informed consent. All experiments were conducted with approval from the University of Newcastle Safety Committee (Safety REF# 25/2016 and R5/2017). Animal experiments were conducted in accordance with the New South Wales Australia Animal Research legislation. Experimental protocol A-2016-605 was reviewed and approved by the University of Newcastle Animal Care and Ethics Committee.

Rhinovirus propagation, purification and quantification

Rhinovirus strain A1 (RV-A1) was originally purified from a clinical isolate (provided by P.A.B. Wark). Rhinovirus strain A16 (RV-A16) was originally purchased from the ATCC (strain 11757). Both strains were grown in RD-ICAM cells and purified as previously described [23, 24].

TLR2 agonist administration and RV-A1 infection for in vivo *mouse models*

6–8-week-old female BALB/c mice from Australian Bioresources (ABR; Moss Vale, Australia) were used for all experiments. Mice were housed in individually ventilated cages with HEPA filtered air and food/water *ad libitum*. All experiments were conducted in a biosafety cabinet under clean conditions. INNA-X was obtained from Ena Respiratory (Melbourne, Australia) in lyophilised form and resuspended in sterile saline. Mice were treated with INNA-X intranasally at the times and doses indicated in the text. Mice were

infected intranasally with RV-A1 (2.5×10^6 median tissue culture infectious dose [$TCID_{50}$]), as previously described [23, 24]. Bronchoalveolar lavage (BAL) and lung samples were harvested 2 days post infection.

BAL cell analysis

Mouse tracheas were cannulated, and lower airways flushed with HBSS (Hyclone; GE Life Sciences, North Ryde (Sydney), Australia). Supernatants were stored at −80°C. Cells were RBC-lysed and leukocyte concentrations determined by haemocytometer count. Cytospins were performed and May-Grunwald +Giemsa staining was used to enumerate neutrophils, lymphocytes and macrophages by microscopy.

RNA isolation and quantitative reverse-transcription (qRT)-PCR

Apical lung lobes were harvested in RNA-Later (Invotrogen branded, licensed through Ambion, supplied by Thermo Fisher Scientific, North Ryde (Sydney), Australia), homogenised in RNeasy lysis buffer (RLT) (Qiagen, Chadstone (Melbourne), Australia) containing 1% β-mercaptoethanol (2ME), cell debris was pelleted and supernatant stored at −80°C. Air–liquid interface (ALI) membranes were vortexed in RLT/2ME, the membrane was removed and the lysate was stored at −80°C. Mouse lung RNA was manually extracted from the RLT lysate using the miRNeasy kit (Qiagen) following the supplier's protocol. ALI RNA was extracted on the QiaCube (Qiagen) using the miRNeasy kit (Qiagen). RNA concentrations were determined by Nanodrop and 200 ng (ALI samples) or 1000 ng (mouse lung) was reverse transcribed. qPCR was performed on an ABI7500 or Quant Studio 6 using TaqMan FAM-TAMRA reagents (Life Technologies/ Thermo Fisher Scientific, North Ryde (Sydney), Australia), mastermix containing ROX (Qiagen), and primer–probe combinations outlined in table S3. Absolute quantification of genes of interest were determined using standards of known concentration. Genes of interest were normalised to the reference gene 18S.

Air-liquid interface of airway epithelial cell cultures

Primary BECs obtained from moderate–severe persistent asthmatic donors were grown until confluent and differentiated at air liquid-interface (ALI), as previously described [25, 26].

BECs obtained from one healthy donor at passage 2 were expanded in submerged monolayer culture using Rho-associated protein kinase (ROCK) inhibitor (final concentration 10 µM) in conjunction with irradiated fibroblast feeder cells. Expanded BECs were maintained in media comprised of 33% DMEM (high glucose +L-glutamine)/67% Ham's F12 containing 5% FCS, hydrocortisone (final concentration 400 $ng{\cdot}mL^{-1}$), insulin (final concentration 5 $\mu g{\cdot}mL^{-1}$), rhEGF (final concentration 10 $ng{\cdot}mL^{-1}$), cholera toxin (final concentration 8.4 $ng{\cdot}mL^{-1}$), adenine (final concentration 23.9 $\mu g{\cdot}mL^{-1}$) and 0.2% penicillin streptomycin [27] and sub-cultured for a further three passages. Once confluent, these BECs were seeded onto polyester transwell membranes and differentiated as previously described [25, 26].

TLR2 agonist dosing and RV inoculation of human ALI BECs

24 h prior to infection, the differentiated epithelium was treated apically with 20 nM INNA-X in BEBM minimal starvation media (Lonza; BEBM+1% ITS and 0.5 lipoteichoic acid). Healthy donor cultures were inoculated with RV-A1 or RV-A16 (multiplicity of infection (MOI) 0.1) for 2 h on the apical culture surface at 35°C. For asthma donor cultures, MOI was 0.001. Following infection, the apical compartment was washed twice with PBS. Starvation media containing TLR2 agonist was then placed in the apical compartment (controls received media alone) at 35°C.

Sample collection from ALI cultures

ALI culture samples were collected at timepoints indicated in the text. Apical media was removed and stored at −80°C for downstream protein analyses. Half of the transwell was collected in RLT buffer (Qiagen) containing 1% 2ME for molecular analyses and half retained for protein analyses in RIPA buffer containing protease inhibitor cocktail (Roche, North Ryde (Sydney), Australia).

Protein quantification by ELISA

Protein levels of airway cytokines were quantified by Duoset ELISA (R&D Systems, Minneapolis, USA) as per manufacturer's instructions for KC/interleukin (IL)-8 (CXCL1) and TNF-α in mouse BAL samples. Duoset ELISA for human IL-29/IL-28B (IFN-λ1/3) (R&D Systems) was used on BEC samples.

Immune transcriptome expression analyses

Purified total RNA was hybridised to the mouse immunology GX code set (Nanostring, Seattle, USA/ Bio-Strategy, Brisbane, Australia) or human immunology panel version 2 (Nanostring), as per manufacturers' instructions. Raw data was quality control checked and normalised based on positive controls, negative controls and housekeeper gene expression for export into Monash-DEGust Voom/Limma platforms of gene expression analyses. Alternatively, raw counts were imported into the Nanostring

advanced analysis platform for automatic normalisation using the gold-standard, inbuilt software GENorm for best housekeeper detection, followed by identification of DEGs and pathway analyses, as outlined in the text.

Statistical analyses

Data from *in vivo* mouse experiments (excluding transcriptome data) were analysed by one-way ANOVA, with Holm–Sidak correction for multiple comparisons. All data from mouse experiments were assessed for normal distribution using a combination of Anderson–Darling, D'Agostino and Pearson, and Shapiro–Wilk tests. Any group that deviated significantly from normal distribution were subsequently analysed using non-parametric Mann–Whitney, or Kruskal–Wallis (with Dunn's correction for multiple comparisons) tests, as indicated in figure legends. All data from healthy control ALI cell cultures were analysed with two-way ANOVA or by one-way ANOVA, with Holm–Sidak correction or Mann–Whitney test. Time course data were assessed by two-way ANOVA with Bonferroni correction for multiple comparisons over time. Friedman test with Dunn's correction for multiple analyses, or Wilcoxon signed rank tests were conducted on data from asthmatic donors due to the assumption of non-parametric nature of data from different human donors. Statistical analyses were performed using Graph Pad Prism 8.3.0 software (La Jolla, CA, USA) with α value of 0.05. Immune transcriptome data was analysed as described in figure legends using either univariate t-test (mouse lung data; nSolver software, Nanostring, Seattle, USA), Benjamini Yekutieli corrected p values (BEC data; nSolver software), false discovery rate (FDR)-corrected p-values (Voom/Limma, Monash DEGust platform, Monash, Australia) or a combination of z-score (nSolver advance analysis platform) with follow-up one-way ANOVA and Holm–Sidak correction (Graph Pad Prism).

Results

INNA-X treatment suppresses rhinovirus infection alone and in combination with corticosteroid

INNA-X is a stable TLR2-specific agonist with suitable characteristics for *in vivo* delivery, developed to negate off-target effects reportedly caused by the cationic lysine moieties of existing TLR2 agonists [28]. INNA-X activated both mouse and human TLR2, inducing downstream NF-κB signalling pathways, detected in an *in vitro* reporter system (figure S1). We compared INNA-X to the commercially-available TLR2-agonist Pam2CysSK4 in an established mouse RV-A1 infection model [23]. Mice were treated intranasally with a single dose of INNA-X or Pam2CysSK4 (at concentrations of both 2 and 10 pmol) 7 days prior to RV-A1 infection. Both drugs (at 10 pmol per mouse) significantly reduced lung viral RNA, whereas only the 2 pmol INNA-X dose significantly reduced lung viral load (figure S2).

We next assessed how INNA-X treatment modulated host resistance to RV-A1 infection. Mice were treated intranasally with low dose INNA-X (2 pmol) alone, or in combination with the inhaled corticosteroid (ICS) fluticasone propionate (FP) (administered 1 h before RV-A1 infection; experimental timeline figure 1a, as previously published) [13]. Endpoints were measured 2 days post infection (9 days post-INNA-X treatment). INNA-X treatment significantly reduced lung viral load by approximately 50%, regardless of corticosteroid treatment (figure 1b, figure S3). In contrast, fluticasone propionate treatment (without INNA-X) significantly increased viral load compared to saline treated, RV-A1 infected mice (figure 1b). In the absence of INNA-X treatment, no significant increase in expression of anti-viral IFN-β or -λ was observed, compared to mock-infected mice (figure 1c and d). Both IFN-β (figure 1c) and IFN-λ (figure 1d) were significantly elevated following INNA-X pre-treatment alone, but not following co-treatment with fluticasone propionate. Thus, INNA-X treatment modulates IFN responses following RV-A1 infection.

ICS treatment or repeated weekly dosing does not affect INNA-X-mediated lymphocyte recruitment or inhibition of virus-induced inflammation

We next quantified inflammatory cell subsets and cytokines in BAL samples. No significant difference in total leukocyte numbers were observed following INNA-X treatment (figure 2a). However, lymphocyte numbers were increased following INNA-X treatment in all groups (including mock-infected mice), compared to saline-treated controls (figure 2a). Increased macrophage numbers were observed only in RV-A1-infected mice treated with both INNA-X and fluticasone propionate (figure 2a). Airway neutrophil numbers were of particular relevance, as neutrophilic airway inflammation is typically associated with the severity of RV-induced disease in humans [23, 29]. RV infection alone in saline-treated mice increased BAL neutrophils, which was unaltered by fluticasone propionate treatment (figure 2a). In contrast, INNA-X treatment significantly reduced neutrophil numbers to baseline levels, regardless of fluticasone propionate co-treatment (figure 2a). To identify potential mechanisms underlying this observation, we quantified relevant chemokines and cytokines. Neutrophil chemokine CXCL1 (mouse IL-8/KC) was reduced following treatment with INNA-X, with the lowest levels observed following treatment with both INNA-X and fluticasone propionate (figure 2b). INNA-X treatment increased TNF-α production in RV-A1-infected mice by approximately 30%, which was inhibited by fluticasone propionate co-treatment

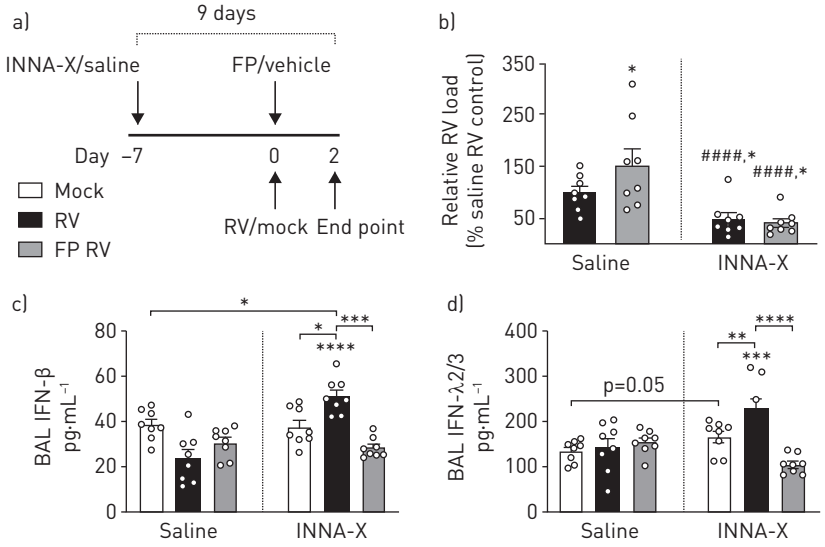

FIGURE 1 INNA-X treatment *in vivo* reduces lung viral load in combination with corticosteroid treatment. a) Experimental timeline. Mice were treated 7 days before RV-A1 infection and samples collected 2 days after infection. For mock infected mice, samples were collected 9 days after INNA-X treatment. Some groups were treated with fluticasone propionate (FP) prior to infection. b) RV-A1 RNA levels in lung tissue. c) Interferon (IFN)-β and (d) IFN-λ2/3 protein levels in BAL samples. Data represent mean±SEM, n=8 mice per group, representative of at least two independent experiments. *: p<0.05; **: p<0.01; ***: p<0.001; ****: p<0.0001, one-way ANOVA with Holm–Sidak's correction for multiple comparisons, compared with saline RV control (unless indicated otherwise). ####: p<0.0001 one-way ANOVA with Holm–Sidak's correction for multiple comparisons, compared to saline FP RV.

(figure 2b). In summary, INNA-X treatment promoted lymphocyte recruitment, inhibited RV-induced neutrophilic inflammation, further supported by ICS co-treatment.

We also assessed viral load and airway CXCL1 levels following RV-A1 infection in mice prophylactically treated with multiple doses of INNA-X administered weekly, for 2 or 3 weeks (to model a potential prophylactic treatment strategy). Repeated weekly INNA-X treatment reduced lung viral load, either alone or with fluticasone propionate co-treatment (figure 2c; figure S3). INNA-X-mediated inhibition of RV-A1-induced CXCL1 expression was also observed following repeated INNA-X treatments (figure 2d).

Timing of TLR2 agonist alters specific gene expression patterns of innate immune priming

To understand the mechanisms mediating INNA-X-induced protection, we characterised the lung tissue immune transcriptome using Nanostring technology. Two treatment protocols were compared, with outcomes assessed either 9 days or 3 days after INNA-X treatment. Mice were infected either 7 days or 1 day after INNA-X treatment (figure 3a). Both treatment protocols significantly reduced lung RV-A1 levels assessed 2 days post infection, demonstrating that INNA-X treatment 1 day before infection was also effective (figure 3b). To clarify mechanisms, differentially expressed genes (DEGs) in lung tissue were visualised using Voom/Limma software [30]. Clusters of DEGs were also visualised using Euclidean hierarchy clustering in Heatmapper software [31] (figure 3c). In uninfected mice, multiple CC and CXC chemokine genes were up-regulated at both 9 and 3 days post-INNA-X treatment. In RV-A1-infected mice, we noted two distinct gene expression patterns in response to virus infection, which differed depending on the timing of INNA-X treatment. Treatment with INNA-X 1 day before infection augmented host lung tissue immune responses, exemplified by up-regulation of two gene clusters (designated clusters 1 and 2). Up-regulated clusters were enriched for anti-viral/interferon stimulated genes (IFI204, IRF7, MX1, IFIT2) and multiple CC and CXC chemokines (figure 3c). This response was associated with increased lymphocyte numbers and elevated CXCL1 levels in BAL samples (figure S4). This heightened lung tissue immune response was not apparent following treatment 7 days before infection. Rather, there was a general reduction in lung tissue immune gene expression following treatment 7 days before infection, compared to the untreated (saline) RV-A1-infected group. Gene clusters 1 and 2 highlighted a diminished immune signature in lung tissue 9 days post-treatment in the RV-A1-infected group (figure 3c).

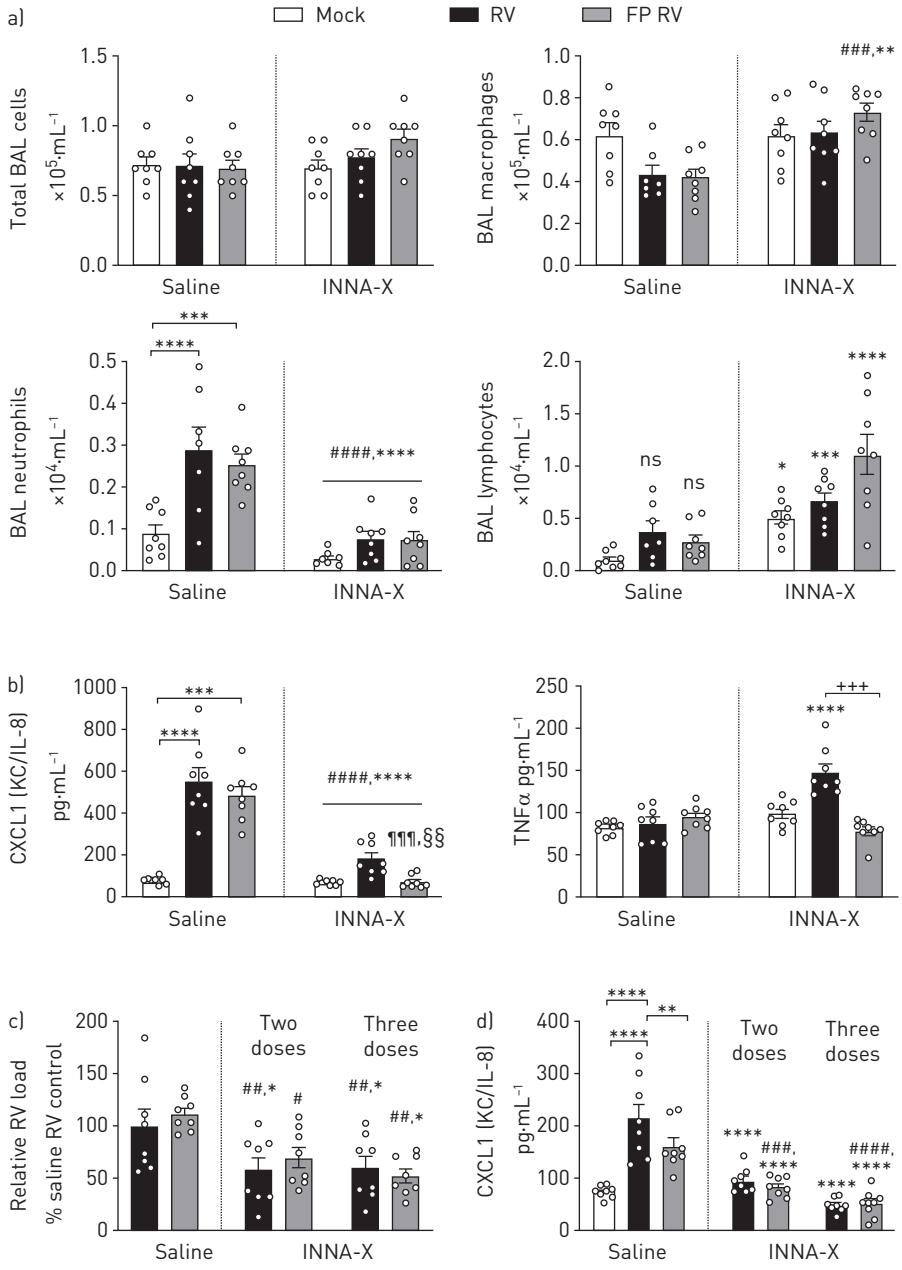

FIGURE 2 INNA-X treatment *in vivo* inhibited rhinovirus-induced neutrophilic inflammation and promoted lymphocyte recruitment. Mice were treated 7 days before RV-A1 infection and samples collected 2 days after infection. For mock infected mice, samples collected 9 days after INNA-X treatment. Some groups were treated with fluticasone propionate (FP) prior to infection. a) Total cell numbers and differential, macrophage, neutrophil and lymphocyte counts in bronchoalveolar lavage (BAL). b) Protein levels of BAL cytokines CXCL1 and TNF-α. In separate experiments, mice were treated on day-21, and/or -14, and -7 with INNA-X followed by FP/vehicle treatment and RV/mock infection as previous and samples were harvested 2 days after infection to determine levels of c) RV-A1 RNA in the apical lung lobe and d) BAL CXCL1 protein. Data represent Mean±SEM, n=8 mice per group, representative of at least two independent experiments. *: p<0.05; **: p<0.01; ***: p<0.001; ****: p<0.0001, one-way ANOVA with Holm–Sidak's correction for multiple comparisons, compared with saline RV control (unless indicated otherwise). $^{\#}$: p<0.05; $^{\#\#}$: p<0.01; $^{\#\#\#}$: p<0.001; $^{\#\#\#\#}$: p<0.0001 one-way ANOVA with Holm–Sidak's correction for multiple comparisons, compared to saline FP RV. $^{+++}$: p<0.001 by Mann–Whitney. ¶¶¶: p<0.001 compared with saline RV control; §§: p<0.01 compared with saline FP RV by Kruskal–Wallis with Dunn's correction for multiple comparisons. "ns" denotes not significant (p>0.05).

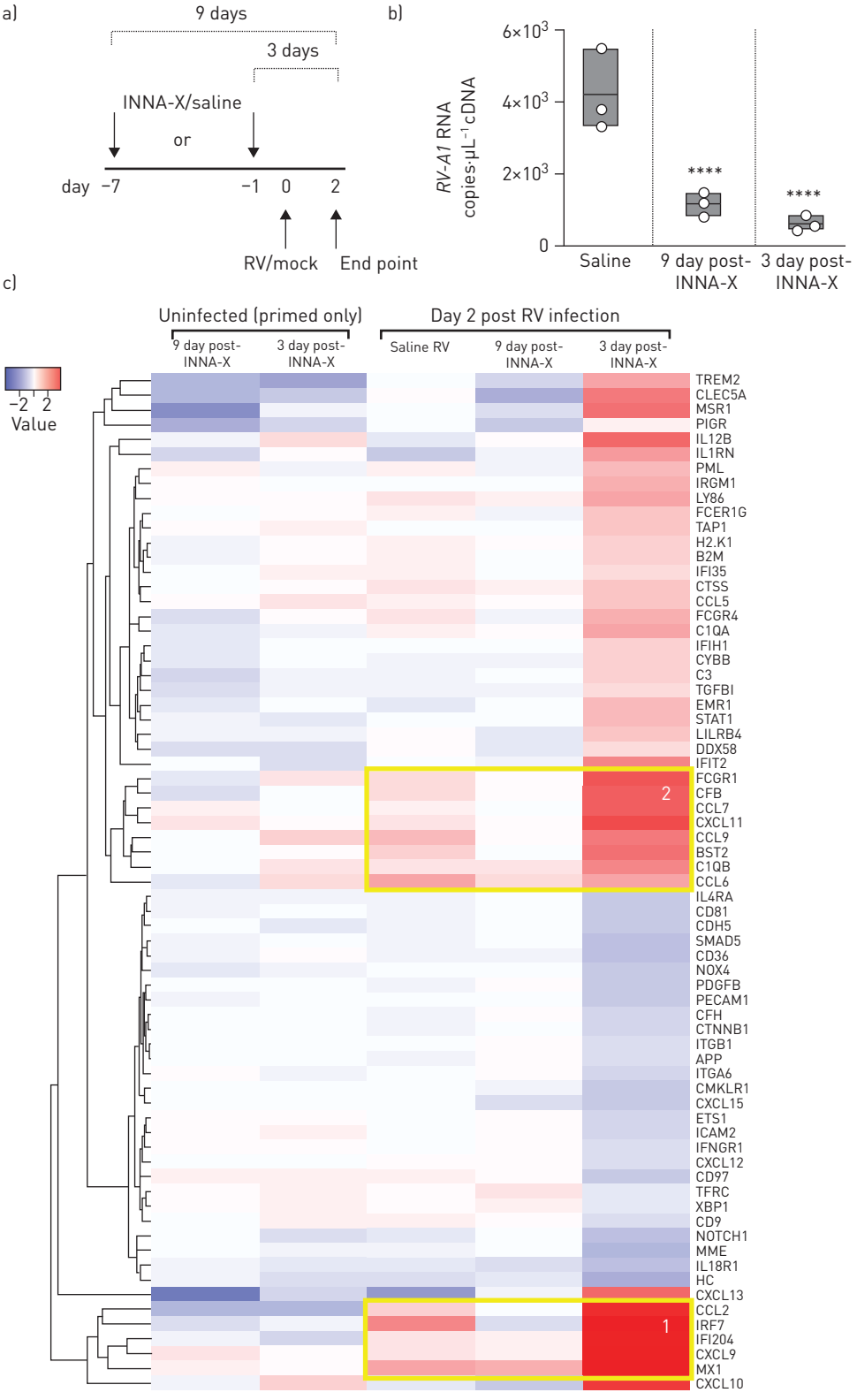

FIGURE 3 INNA-X treatment *in vivo* is associated gene expression patterns showing enhanced antiviral responses and innate immune system activation. a) Experimental timeline. Mice were treated 7 days or 1 day before RV-A1 infection and samples collected 2 days after infection. For mock infected mice, samples were collected at 3 days- or 9 days after INNA-X treatment. b) RV-A1 RNA in the apical lung lobe. c) Heatmap representation and Euclidean clustering of differentially expressed genes identified by Voom/Limma analysis (FDR p value <0.01) of Nanostring RNA expression. n=3 mice per group.

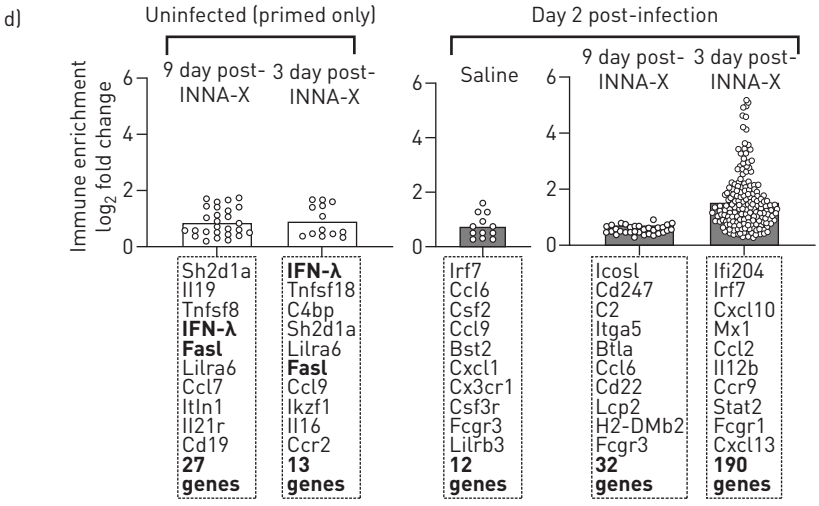

FIGURE 3 Continued. d) Up-regulated gene scores generated using nSolver software (p value filter <0.05). n=3 mice per group.

To better understand the distinct, treatment timing-related profiles observed, we used Nanostring nSolver software to interrogate all up-regulated genes (figure 3d; 10 most highly up-regulated genes listed for each group). In uninfected mice at both 9 and 3 days post-INNA-X treatment, we observed low-level innate immune priming defined by expression of IFN-λ and pro-apoptotic Fas ligand (Fasl) genes. Chemokines CCL7 and CCL9 identified in the Voom/Limma analysis were also identified by the nSolver software, significantly up-regulated in INNA-X-treated mice. We detected twice as many up-regulated genes in lungs harvested 9 days post-agonist treatment compared to 3 days post-treatment in uninfected mice. In RV-A1-infected mice, INNA-X treatment 1 day before infection significantly up-regulated 190 genes. The most highly induced genes identified were IFN stimulated, antiviral molecules Ifi204, IRF7, CXCL10, MX1, STAT2 and chemokines CCL2 and CXCL13. A different gene expression profile was observed with INNA-X treatment 7 days before infection. We observed low-level (less than two-fold) up-regulation of 32 genes (compared with 12 genes in saline-treated mice), which were associated with lymphocyte responses (*e.g.* ICOS ligand, BTLA), chemokines (CCL6) and adaptive immunity (figure 3d). The full lists of up-regulated genes are included in supplementary data file S1. Thus, the presence of chemokines 3 days post-treatment and evidence of modulated lymphocyte regulation 9 days post-treatment were consistent with the observed patterns of lymphocyte recruitment.

INNA-X primed responses against RV-A1 infection in differentiated human primary BECs

To define which aspects of INNA-X treatment effects were mediated by epithelial cells, we assessed TLR2 agonist pre-treatment on RV-A1 infection in differentiated primary human BECs *in vitro*. Differentiated healthy donor BECs [27] were pre-treated with INNA-X 24 h prior to RV-A1 infection. The primary aim of these experiments was to identify the mechanism of action (MOA) of INNA-X in a differentiated primary human BEC–RV infection model [13, 32]. Using BECs from a healthy donor we assessed a time-course of viral load and expression of immune genes using Nanostring human immunology panel with n=1 well per timepoint per treatment. INNA-X suppressed viral load from 24 h to 48 h post-infection (figure S5). Nanostring-based immune transcriptomic analysis revealed evidence of innate immune priming with greater than three-fold up-regulated expression of IDO-1, β-defensin (DEFβ-2) and M-CSF, compared to untreated cells at 24 h post INNA-X treatment. This preceded an accelerated response to RV infection defined by 26 up-regulated genes at 8 h post-infection in INNA-X treated samples, compared with one gene in untreated RV-A1-infected cells. The augmented INNA-X-induced response was evident at 24 h post infection. However, by 48 h post infection, a greater number of genes (enriched for IFN/interferon stimulated genes (ISGs)) were upregulated in untreated cells. This data indicated that INNA-X treatment improves early control of virus infection, reducing the magnitude of later IFN-driven responses (figure S5). To confirm this result in BECs isolated from a different healthy donor with a greater number of experimental replicates per treatment per timepoint, we used conditional reprogramming (CR) to expand BEC numbers to repeat the study n=5 times. Again, responses were analysed prior to and after infection (treatment timeline with viral load shown in figure 4a). INNA-X treatment had no effect on epithelial barrier function, determined by trans-epithelial electrical resistance (TER) (figure S6a).

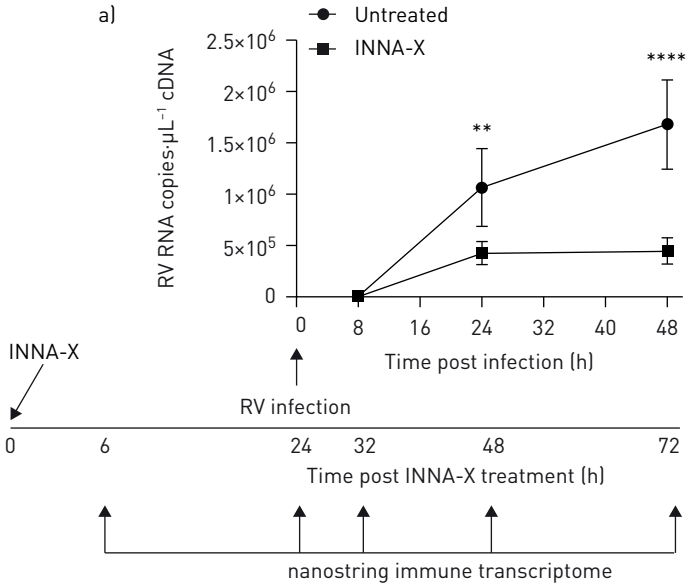

FIGURE 4 INNA-X treatment *in vitro* reduced viral load and enhanced rapid innate immune response in differentiated human bronchial epithelial cell cultures. a) Timeline showing all timepoints of harvest following INNA-X treatment and reduced RV-A1 RNA expression at 8, 24 and 48 h post infection, in differentiated BECs from a healthy donor, with drug treatment 1 day prior to infection. n=5 repeats, mean±SD. **: p<0.01; ****: p<0.0001 by two-way ANOVA with Sidak's correction for multiple comparisons.

INNA-X treatment significantly suppressed viral load, which was evident 24 h post-infection and more apparent after 48 h (figure 4a). Immune transcriptome analysis using the Nanostring human immunology panel (594 genes total) identified three distinct clusters of DEGs encoding molecules enriched for NF-κB-regulated cytokines/chemokines, TNF superfamily/apoptosis and anti-microbial peptides (figure 4b; denoted by blue boxes 1–3). Upregulated DEGs in these clusters at 6 h and 24 h after INNA-X treatment defined a rapid response to RV-A1 infection observed at 8 h after infection (figure 4b). At 48 h post-infection two different DEG clusters were evident, representing anti-viral genes (including type I/III IFNs; figure 4b; denoted by yellow boxes 1 and 2). We noted that type I (IFN-β) and type III IFN-λs (IL28A/B, IL29) were less up-regulated in INNA-X-treated cells at the later timepoint, consistent with a more efficient early innate response and subsequent viral clearance.

To visualise the kinetics of INNA-X-induced gene up-regulation in RV-A1-infected BECs, we plotted the total number of significantly up-regulated genes (statistically significant; greater than three-fold) over time, as well as expression levels relative to untreated and uninfected cells (figure 5a). These results are presented as immune enrichment, defined as the number of upregulated genes (dot points) and the magnitude of gene expression for each gene (height of each datapoint). The response to INNA-X alone (prior to infection) was enriched for NF-κB-regulated anti-microbial genes and chemokines; many of which were subsequently up-regulated 8 h post infection. At this timepoint, INNA-X-primed BECs significantly up-regulated 12 genes (greater than three-fold) in response to RV-A1 infection, whereas untreated RV-A1-infected BECs had no alterations in gene expression (*i.e.* 0 genes up-regulated greater than three-fold; figure 5b). This response persisted through to 24 h post infection (with 11 genes up-regulated after INNA-X treatment *versus* five genes in untreated RV-A1-infected cells; figure 5b). By 48 h post infection up-regulation of numerous interferon-stimulated genes was evident, with untreated RV-A1-infected BECs exhibiting similar gene expression profiles to INNA-X-treated cells. However, the magnitude and number of up-regulated anti-viral genes were higher in untreated, RV-A1-infected cells compared to the INNA-X treated samples (figure 5b). The full lists of upregulated genes are included in supplementary data file S2.

IFN-λ was associated with the accelerated response to rhinovirus after INNA-X treatment

Nanostring-based pathway analyses identified increased "defence response" scores (24 genes; table S2) in INNA-X-treated BECs. The increased defence response score primed in uninfected cells at 6 h and 24 h post-INNA-X treatment, translated to a heightened defence response during RV-A1 infection. In contrast,

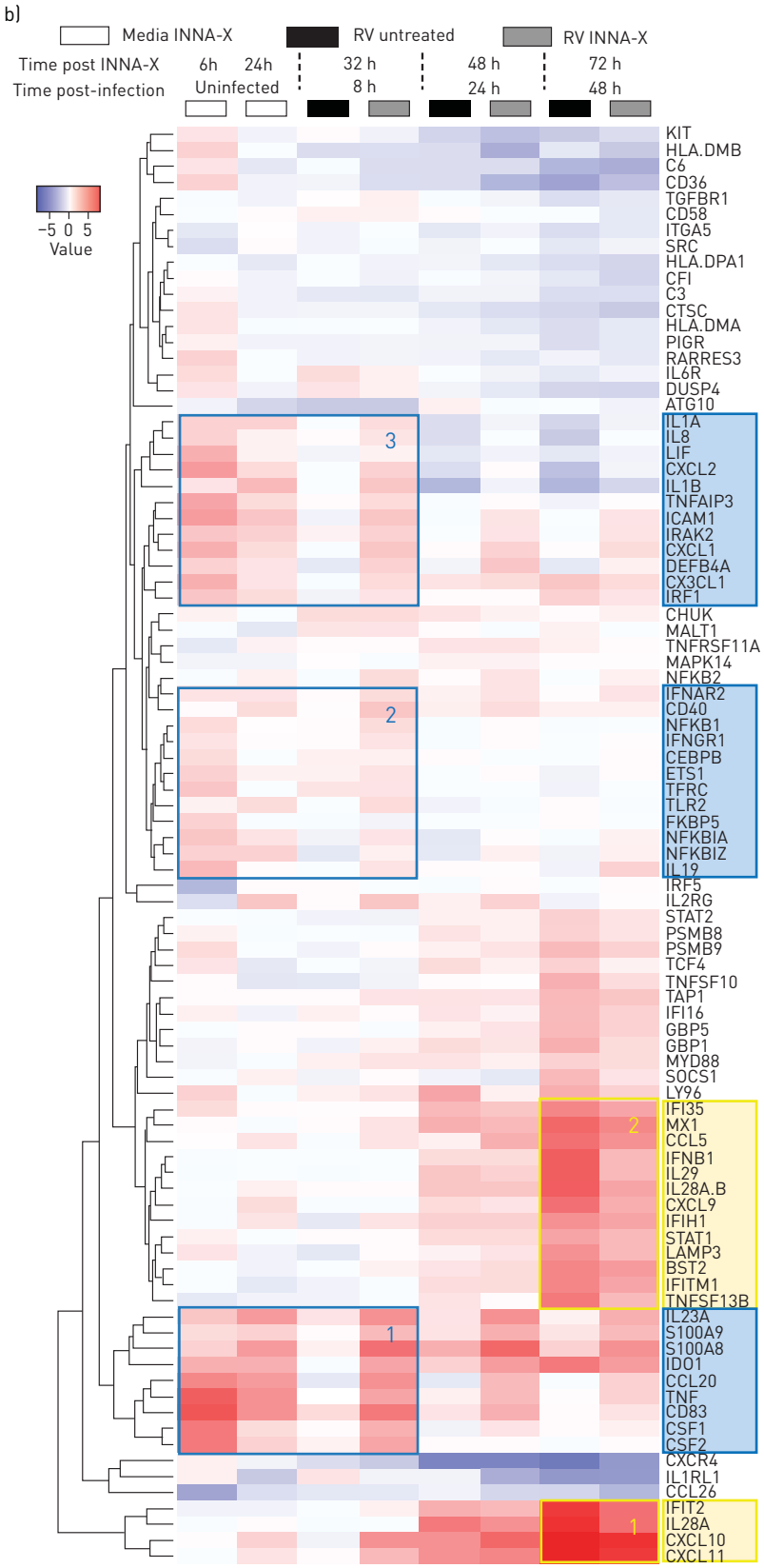

FIGURE 4 Continued. b) Euclidean clustered heatmap of differentially expressed genes identified by Voom/Limma analysis (filtered by FDR p-value <0.001) where NF-κB innate immune priming clusters are denoted in blue (DEG1, 2, 3) and interferon/interferon stimulated gene (ISG)-enriched clusters are denoted in yellow. n=5 repeats.

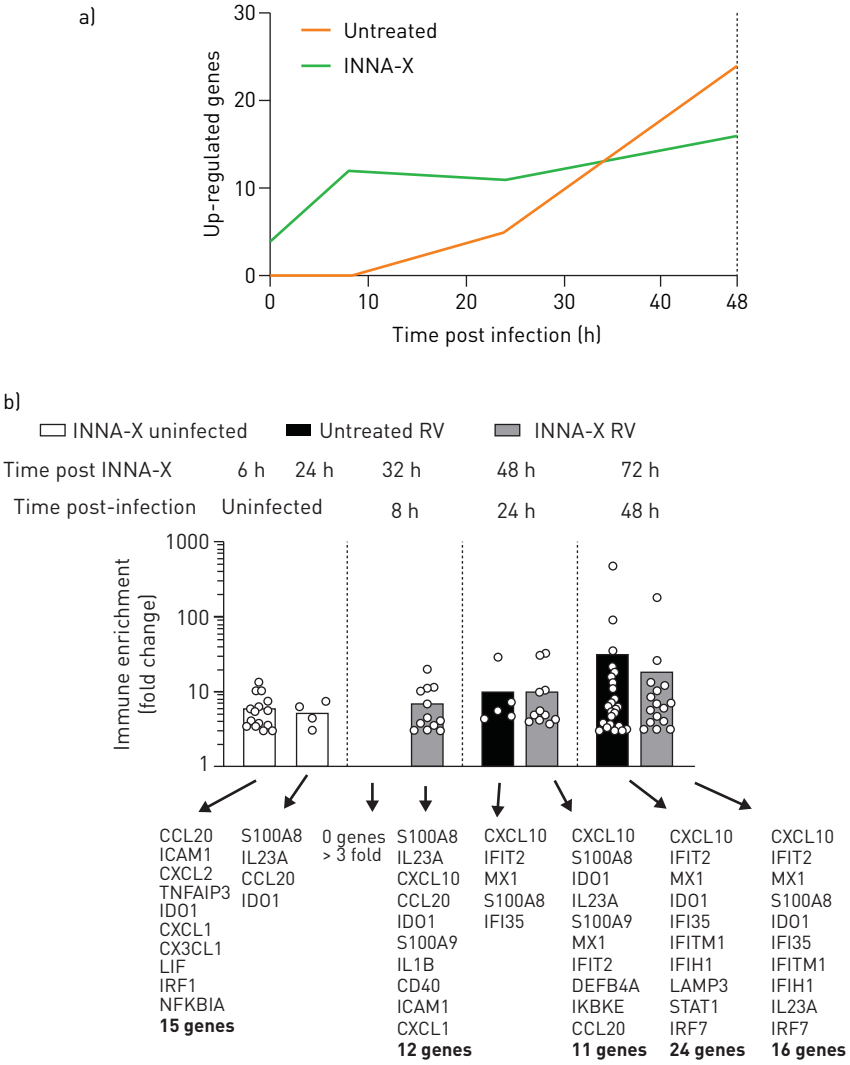

FIGURE 5 INNA-X treatment *in vitro* increased anti-viral gene expression pathways in differentiated human bronchial epithelial cell cultures. a) Kinetics of up-regulated genes (>3-fold by Nanostring) in differentiated BECs from a healthy donor following RV-A1 infection with prior INNA-X treatment. b) Immune enrichment (number and magnitude of up-regulated genes) following treatment of INNA-X and/or infection with RV-A1, determined by Nanostring with the 10 most highly expressed genes listed in order below the x-axis. Data was filtered by Benjamini Yekutieli corrected p values <0.05. n=5 repeats.

there were no net increase in defence score evident in untreated, RV-A1-infected cells highlighting the potential to therapeutically increase the innate immune responsiveness of BECs (figure 6a). This translated to a more effective response to infection; at 8 h post infection there remained a heightened defence response score in INNA-X treated cells which was associated with lower viral load at this time (figure 6b).

Type I/III interferons were not included in the "defence response" pathway gene set, so we also quantified these relevant genes independently using qPCR. *IFN-β* mRNA was not consistently up-regulated by INNA-X treatment following RV-A1 infection (figure 6c). In contrast, *IFN-λ1* expression was significantly increased by INNA-X treatment, and near significant (p=0.055) increased *IFN-λ2/3* expression (figure 6d).

We also assessed the efficacy of INNA-X treatment on infection by a major group rhinovirus strain RV-A16 in ALI-differentiated primary human BECs from a healthy donor, CR-expanded to provide sufficient cells for n=5 repeats. INNA-X treatment significantly suppressed RV-A16 viral load after 48 h (figure 7a). Again, no upregulation of *IFN-β* mRNA was observed at 24 h post-INNA-X treatment as well as after infection (figure 7b), while *IFN-λ1* and *IFN-λ2/3* expression were significantly increased by

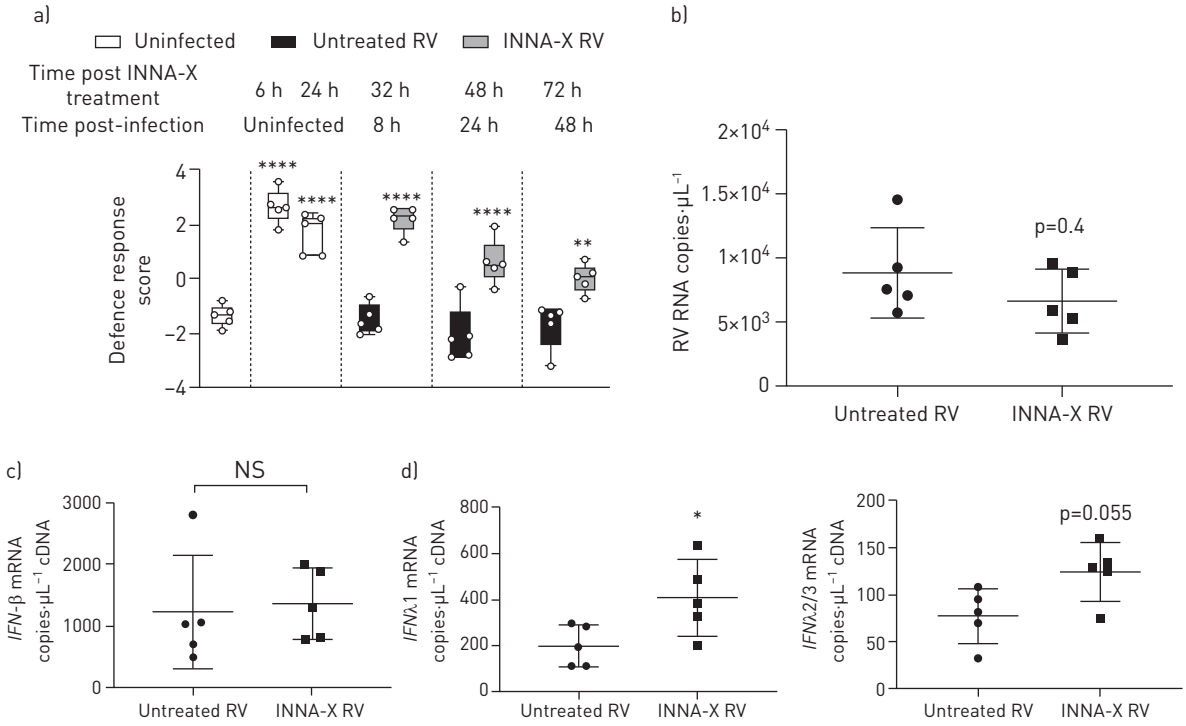

FIGURE 6 INNA-X treatment *in vitro* enhanced defence response pathway scores and early epithelial IFN-λ responses to RV-A1 infection. a) Timeline showing enriched defence response scores (defined by Nanostring advanced analysis platform of gene expression) following INNA-X treatment 6 and 24 h post INNA-X treatment and in INNA-X treated cells, 8, 24 and 48 h post infection, in differentiated BECs from a healthy donor. RNA expression at 8 h post infection of b) RV-A1, c) IFN-β, and d) IFN-λ1 and IFNλ2/3. n=5, mean±SD (b–d). Data analysed by one-way ANOVA with Holm-Sidak's correction for multiple analyses (a) or by Mann Whitney test (b–d). *: p<0.05; **: p<0.01; ****: p<0.0001 compared to the relevant untreated control.

INNA-X treatment (INNA-X primed) as well as by 24 h post infection (figure 7c). INNA-X treatment also significantly increased expression of the ISGs *viperin* at 24 h post infection and *OAS1* at 8 h post infection, with a trend towards increased *PKR* noted at 24 h post infection (figure 7d).

INNA-X boosted anti-viral responses in RV-infected BECs from patients with asthma

We previously developed a low MOI RV-A1-infection model using BECs isolated from donors with asthma, which identified delayed RV-induced anti-viral immune responses beyond 24 h post infection, compared with cultures from healthy controls [32]. We applied this model to determine whether INNA-X treatment also effectively inhibits RV-A1 infection, in the context of intrinsic innate immune deficiency (*i.e.* asthma). INNA-X treatment of differentiated BEC cultures derived from eight donors with asthma did not affect barrier function (figure S6b). Pre-treatment with INNA-X significantly reduced viral load at 48 h post infection, compared to untreated controls (figure 8a). Increased *IFN-β* expression was not a feature of the INNA-X response at 24 h post treatment in uninfected cells (figure 8b). However, INNA-X pre-treatment increased *IFN-β* levels at 8 h post RV infection/mock infection, which further increased by 24 h post infection/mock infection (figure 8b). As previously reported [32], untreated RV-infected BECs from asthma donors failed to induce IFN-β 24 h post-infection (figure 8b). INNA-X pre-treatment significantly increased both type III IFN-λ1 and IFN-λ2/3 gene expression and boosted the IFN-λ response to RV-A1. INNA-X also increased IFN-λ1 expression in uninfected cells at 24 h post-infection. Infection alone did not induce IFN-λ gene expression in untreated cells (figure 8c). Enhanced IFN-λ expression 8 h after INNA-X treatment did not correspond to significantly increased IFN-λ protein production 96 h post infection (figure 8d), suggesting that low-level, early expression (rather than prolonged IFN-λ production) was associated with the protective effects of INNA-X treatment. INNA-X treatment led to significant expression of the ISGs *viperin* and *OAS1*, with a trend towards increased *PKR*, 8 h post infection in RV-A1-infected cultures, whereas untreated, RV-A1-infected cells did not mount a significant response (figure 8e).

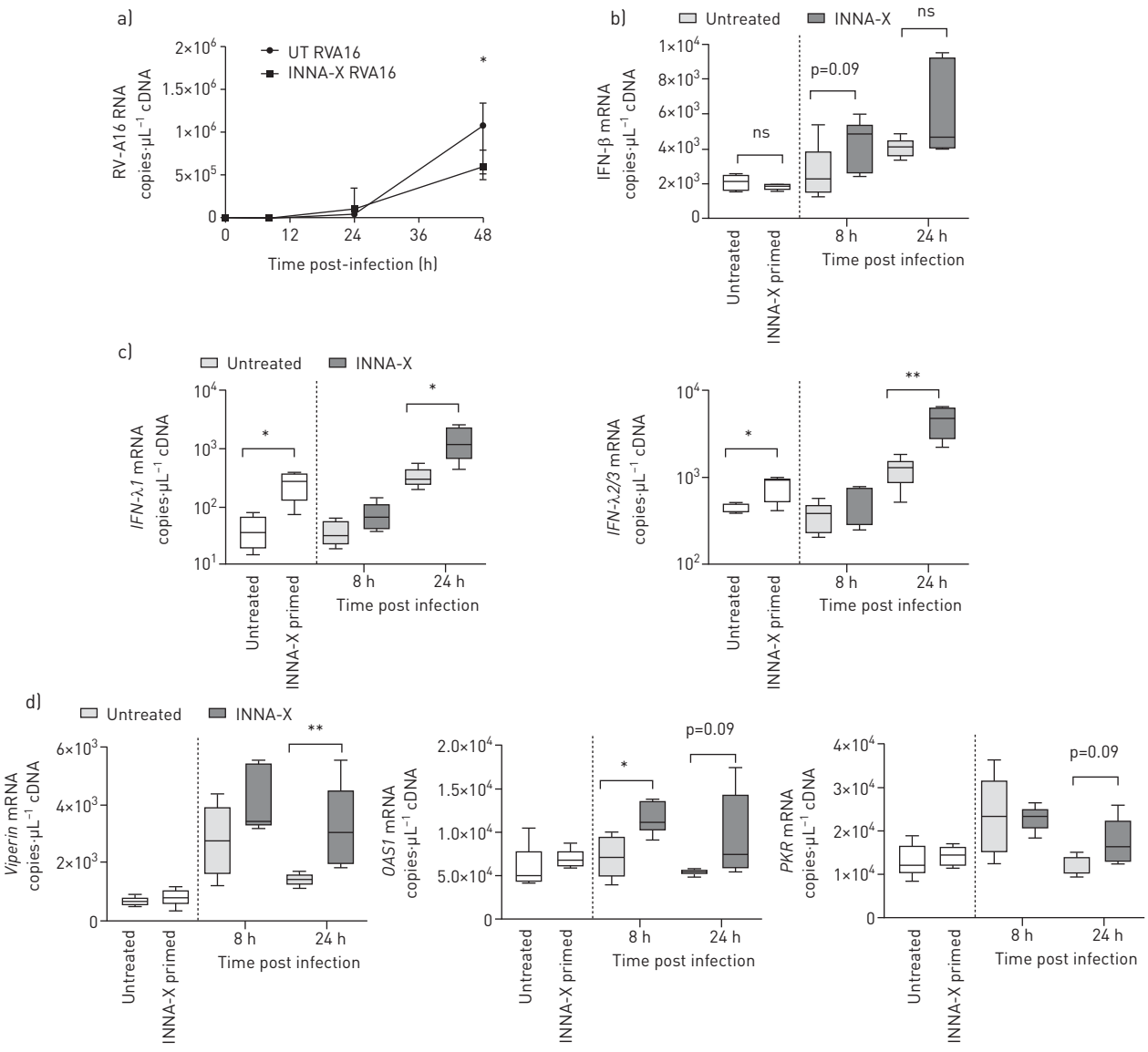

FIGURE 7 INNA-X treatment *in vitro* reduced viral load and enhanced early epithelial IFN-λ responses to RV-A16 infection. RNA expression of a) RV-A16, b) IFN-β, and c) IFN-λ gene expression at 8 and 24 h post infection in differentiated BECs from a healthy donor (boxplots showing median and 5%–95% percentiles). d) RNA expression of ISGs (Viperin, OAS1, PKR) at 8 and 24 h post infection. Data analysed by two-way ANOVA with Holm-Sidak's correction for multiple analyses (a) or by Mann Whitney test (b–d). *: p<0.05; **: p<0.01 compared to the relevant untreated control. n=5 repeats.

Discussion

Cell-surface TLRs, such as TLR2, recognise a diverse range of microbial molecules and there is a growing body of evidence that cell-surface TLRs are activated by viruses. This led us to investigate whether TLR2 stimulation could promote respiratory epithelial immune responses to RV infection.

The present study provides three significant developments. Firstly, we show that a single dose of INNA-X treatment can promote resistance to viral infection for at least 7 days. We provide evidence that this effect is achieved by promoting rapid and sustained innate immune activation. Secondly, we provide evidence that INNA-X-induced protection against RV-A1 infection is maintained when administered in combination with ICS (specifically fluticasone propionate). Patient groups at the most risk of RV-induced respiratory disease (*e.g.* people with asthma and COPD) are typically treated with regular maintenance ICS [33], and ICS treatments (including with fluticasone propionate) suppress anti-viral and anti-microbial immunity [13, 34, 35]. In fact, we observed that ICS treatment reduced INNA-X-enhanced levels of TNF-α, IFN-β

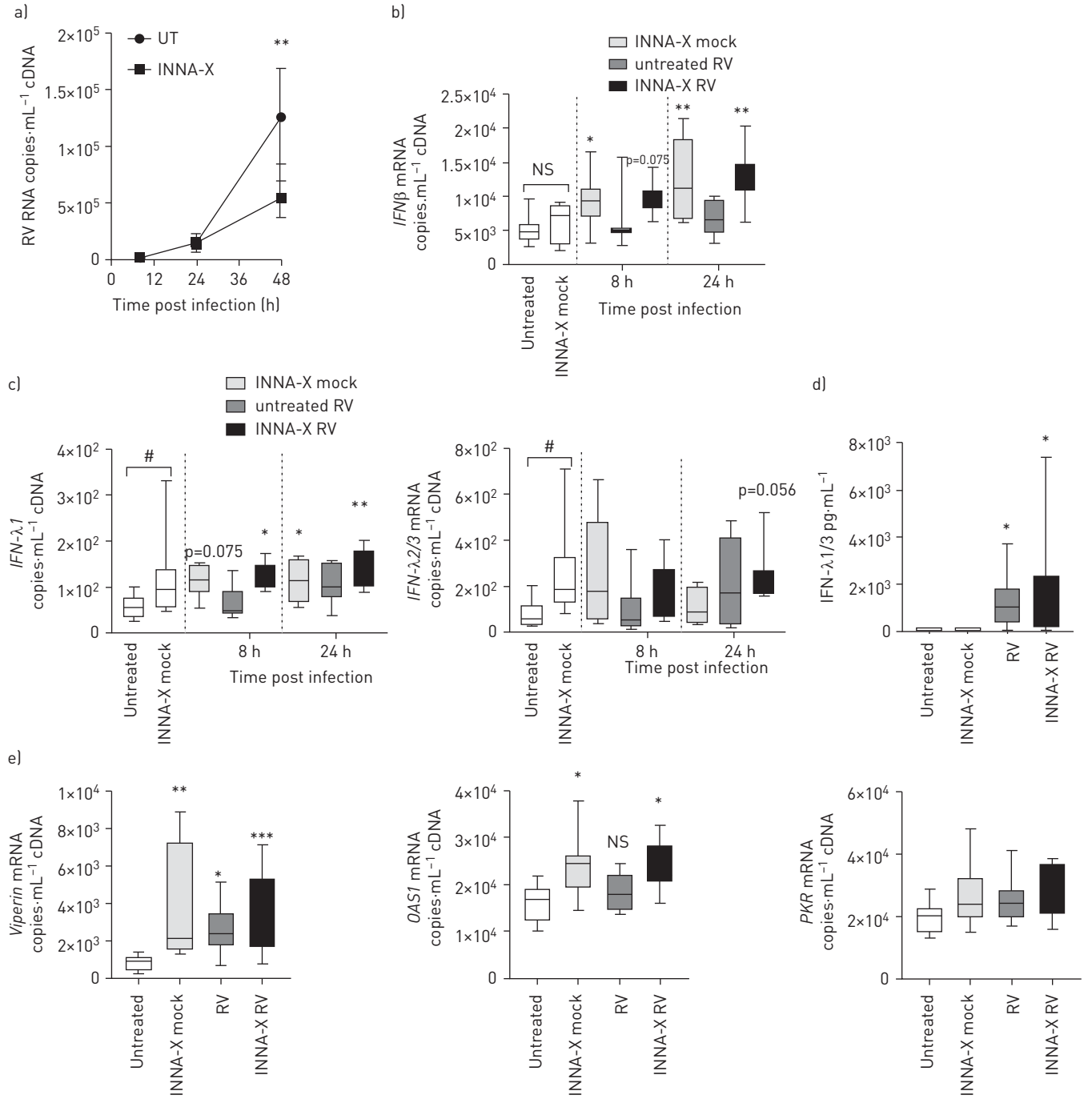

FIGURE 8 INNA-X treatment *in vitro* primed resistance to RV-A1 infection in differentiated human bronchial epithelial cells from asthmatic donors. RNA expression of a) RV-A1, b) IFN-β, and c) IFN-λ gene expression at 0, 8 and 24 h post infection, and d) protein levels in apical supernatant at 96 h post infection. e) ISGs (Viperin, OAS1, PKR) RNA expression at 8 h post infection. n=8 donors with persistent moderate to severe asthma, median (interquartile range) (a) or boxplots showing median and 5%–95% percentiles (b–e). Data analysed by two-way ANOVA with Bonferroni correction (a), Friedman test with Dunn's correction ((b–d) denoted by asterisks) or Wilcoxon signed rank test (#, uninfected comparison). *: p<0.05, **: p<0.01, ***: p<0.001 (by Friedman test) compared to untreated control. #: p<0.05 compared to untreated control by Wilcoxon signed rank test.

and IFN-λ, without altering protection from RV infection. This is evidence that INNA-X treatment could be an effective add-on therapy to ICS by supporting anti-viral immunity without requiring increased IFN production. Thirdly, INNA-X-mediated protection was achieved in asthma donor-derived epithelial cell cultures. Intrinsic deficiencies in epithelial innate immunity in asthma have been associated with susceptibility to viral infection [20–22], which we have shown is in part due to epithelial cell-intrinsic

delayed innate immune responses [32]. We confirm that BECs from asthma donors failed to induce expression of IFNs 24 h post infection [32]. However, pre-treatment with INNA-X primed epithelial cells to respond to RV-A1 and significantly increased expression of IFN-β and IFN-λ by this time. This was associated with decreased RV-A1 viral load.

The duration of effect of INNA-X treatment we observed is consistent with findings by Tan *et al.* [18], who observed enhanced influenza clearance in mice treated with TLR2 agonists 7 days prior to infection and for the first time (to our knowledge) we show that this is due to sustained low-level innate immune activation, leading to an enhanced/accelerated response to viral infection and decreased viral load (*i.e.* "innate immune priming"). To better understand the timing effects, we compared pre-treatment 7-days before infection to 1-day before infection. This identified two mechanisms of action depending on timing of INNA-X administration relative to viral infection. Treatment 7-days prior to RV-A1 infection reduced the magnitude of lung tissue immune gene expression, compared to RV-A1 infection alone. In contrast, treatment 1-day before infection led to robust enrichment of genes involved in the anti-RV response. Despite differing effects on gene expression, both treatment timings significantly suppressed viral load. We conclude that when RV infection does not occur immediately following agonist treatment (within approximately 1-day), the respiratory mucosa is primed *via* chemokine-mediated recruitment of lymphocytes, which mediate the protective response against RV. In support of this, numbers of up-regulated immune genes were greater 9-days post-treatment compared to 3-days post-treatment, consistent with the time required to establish a network of mucosal lymphocytes that support persistent protection [36]. Further, genes associated with lymphocyte regulation were increased following the earlier INNA-X treatment (*e.g.* BTLA [37] and ICOSL [38]). In line with this, elevated lymphocyte numbers were consistently observed following INNA-X treatment in airway lavage. Furthermore, TLR2 agonist treatment 3-days prior to infection with PR8 (a highly virulent strain of influenza in mice) increased monocyte, macrophage, neutrophil and dendritic cell numbers [39], emphasising the importance of cell-mediated long-term innate immune priming for protection from viral infection.

In mechanism of action experiments with differentiated BEC cultures derived from healthy donors, INNA-X treatment triggered low-level innate immune activation prior to RV infection, with up-regulation of NF-κB-regulated genes and a rapid response to RV infection. This response was defined by two distinct waves of innate immune activation by cluster analysis. INNA-X treatment alone increased expression of NF-κB-regulated genes encoding cytokines (*e.g.* IL-1β), chemokines (*e.g.* CXCL1, CXCL2) [40] and anti-microbial molecules (*e.g.* IDO1 [41], calprotectin/S100A8-S100A9 [42]) and these genes were subsequently upregulated 8 h post RV-infection with prior INNA-X treatment. This early response was completely absent in untreated, RV-infected cells. The second wave occurred 24–48 h post infection in INNA-X treated cells and was enriched for expression of interferon-stimulated genes (ISGs). It was evident that by 48 h post infection, untreated cells up-regulated more genes (dominated by ISGs) than INNA-X-treated cells, and that these genes were up-regulated to a higher magnitude also. The decreased magnitude of gene expression in INNA-X treated cells was also observed in the ISG clusters in the heatmap data. We propose that this observation likely results from lower viral load from 24 h post infection onwards after INNA-X treatment, leading to a decreased activation of the late IFN-mediated response. Overall, the data is consistent with an INNA-X-induced early immune priming response, resulting in accelerated response to RV-A1, a minor group, low density lipoprotein receptor (LDLR)-binding subtype. INNA-X treatment of BECs transiently increased ICAM-1 gene expression prompting investigation of major group (ICAM-1 binding) RV-A16. Following infection with RV-A16, we also observed suppression of viral load with enhanced type III IFN and ISG responses (Viperin and OAS), confirming INNA-X efficacy against a major group (ICAM-1 binding) RV subtype.

Myristoylated (Myr) RV capsid VP4 interacts with TLR2 and induces pro-inflammatory cytokine gene expression [43]. We did not see evidence of rhinovirus-induced TLR2 activation in untreated cells at 8 h post infection and suggest the low multiplicity of infection in our studies likely restricted early exposure to viral MyrVP4 such that it was insufficient to activate TLR2. INNA-X-mediated TLR2 priming may have reduced the threshold for TLR2 activation such that low-level MyrVP4 exposure early during infection was now able to stimulate innate immunity. We also observed upregulated expression of TLR2 itself in our gene expression assessment (NF-κB blue cluster 2; figure 4), which may affect the threshold for activation. In support of this, the NF-κB gene signatures up-regulated by INNA-X were also associated with enhanced response to RV infection suggesting that INNA-X and RV were activating a common innate immune network.

Other respiratory viruses are potentially amenable to epithelial, cell-surface TLR-primed innate immune resistance. For example, blocking the TLR2 co-receptor cluster of differentiation 14 (CD14) inhibited

influenza immune mediator production by monocytes and macrophages [44] and we have reported protection against influenza virus infection in mice treated with TLR2 agonists [18, 39]. Respiratory syncytial virus (RSV) binds to TLR4 to induce early NF-κB-mediated lung innate immunity [45] and LPS activation of TLR4-TRIF pathway protects against H5N1 influenza virus infection [46]. Data for coronavirus is less clear, however mice lacking TLR4 are more susceptible to the murine coronavirus that causes mouse hepatitis [47]. Thus, there is now a substantial body of evidence to support investigation of the capacity of INNA-X to prime airway epithelial innate immunity against multiple, clinically important respiratory viruses.

We consistently observed early, low-level up-regulation of type III IFN genes encoding IFN-λ1 and IFN-λ2/3, and not type I (IFN-β) in BECs from the healthy donor and patients with asthma. While both type I and type III IFNs are well known for their role in anti-viral immunity *via* endosomal TLR activation, it is now becoming clear that type III IFNs can also be induced by cell-surface, bacteria-sensing TLRs and have an important function in epithelial barrier and innate immune homeostasis [48]. From a clinical/host-fitness perspective, early low-level expression of IFN-λs *versus* protracted, high-level expression of type I/III IFNs is desirable and indicative of a more efficient, early control of infection. This concept was elegantly defined by Galani *et al.* [49], who used influenza infection studies to show that IFN-λs are the first IFNs produced and underpin airway epithelial frontline protection.

In summary, we show that prophylactic, epithelial activation of TLR2 primes lung innate immunity that boosts the response to RV infection (major- and minor-group viruses). This improved the ability of the epithelium to respond quickly and control viral infection, and with time allowed recruitment of lymphocytes associated with prolonged protection from infection and airway inflammation.

Acknowledgements: We would like to thank Jane Read and Kristy Nichol from the Priority Research Centre for Healthy Lungs, University of Newcastle and Hunter Medical Research Institute, who assisted with cell culture maintenance. We thank Matty Bowman and Michelle McGloin from the Priority Research Centre for Healthy Lungs, University of Newcastle and Hunter Medical Research Institute, for their contributions to sample processing and molecular techniques involved in generating qPCR and ELISA data. We thank the administrative staff of the Priority Research Centre (PRC) for Healthy Lungs and the Bioresources staff from the Hunter Medical Research Institute and the University of Newcastle for providing laboratory space, infrastructure and the work environment.

Author contributions: J. Girkin conducted all mouse and nanostring experiments, performed data analysis and interpretation, graphed the data, drafted and edited the manuscript and contributed to conceptual design of the manuscript. S-L. Loo conducted cell culture experiments, assisted with analysis, interpretation and graphing of cell culture experiments and assisted with drafting the manuscript. C. Esneau conducted cell culture experiments and assisted with molecular analysis. S. Maltby assisted with data interpretation and drafting/editing the manuscript. F. Mercuri was involved in experimental design, project management, data interpretation and editing the manuscript. B. Chua contributed to experimental design, interpretation of nanostring analyses and edited the manuscript. A.T. Reid, P.C. Veerati and C.L. Grainge contributed resources and expertise for the experimental platform using conditionally reprogrammed cells. P.A.B. Wark contributed the platform for ALI-differentiation and the bronchial epithelial cells and provided conceptual input. D. Knight and D. Jackson provided conceptual input and design and reviewed the manuscript. C. Demaison, F. Mercuri, D. Jackson and N.W. Bartlett designed the study, performed data interpretation, edited and finalised the manuscript and secured the funding and resources that made this study possible. N.W. Bartlett also supported figure development and had significant input into data interpretation.

Conflict of interest: J. Girkin reports grants, personal fees for consultancy and non-financial support for travel to meetings from Ena Therapeutics Pty Ltd, during the conduct of the study; and has a patent PCT/AU2018/050295 issued. S-L. Loo reports grants from Ena Therapeutics, during the conduct of the study. C. Esneau has nothing to disclose. S. Maltby has nothing to disclose. F. Mercuri is an employee of Ena Therapeutics, and has a patent PCT/AU2018/050295 pending, and a patent PCT/AU2011/001225 issued. B. Chua is a co-founder and shareholder of Ena Therapeutics Pty Ltd. A.T. Reid has nothing to disclose. P.C. Veerati has nothing to disclose. C.L. Grainge has nothing to disclose. P.A.B. Wark has nothing to disclose. D. Knight reports grants from Boehringer Ingelheim, outside the submitted work. D. Jackson is co-founder and shareholder of Ena Therapeutics Pty. Ltd, and has a patent PCT/AU2018/050295 pending, and a patent PCT/AU2011/001225 issued. C. Demaison is an employee of Ena Therapeutics, and has a patent PCT/AU2018/050295 pending, and a patent PCT/AU2011/001225 issued. N.W. Bartlett reports grants, personal fees for consultancy and other (stock options) from Ena Therapeutics, during the conduct of the study; has a patent PCT/AU2018/050295 issued.

Support statement: This work was funded in partnership between The University of Newcastle and Ena Therapeutics Pty Ltd in conjunction with Innovation Connection Grants from the Australian Government, Department of Industry, Innovation and Science. Funding information for this article has been deposited with the Crossref Funder Registry.

References

1 Morikawa S, Kohdera U, Hosaka T, *et al.* Seasonal variations of respiratory viruses and etiology of human rhinovirus infection in children. *J Clin Virol* 2015; 73: 14–19.
2 Visseaux B, Burdet C, Voiriot G, *et al.* Prevalence of respiratory viruses among adults, by season, age, respiratory tract region and type of medical unit in Paris, France, from 2011 to 2016. *PLoS One* 2017; 12: e0180888.
3 Papadopoulos NG, Bates PJ, Bardin PG, *et al.* Rhinoviruses infect the lower airways. *J Infect Dis* 2000; 181: 1875–1884.
4 Gern JE, Busse WW. Association of rhinovirus infections with asthma. *Clin Microbiol Rev* 1999; 12: 9–18.
5 McManus TE, Marley AM, Baxter N, *et al.* Respiratory viral infection in exacerbations of COPD. *Respir Med* 2008; 102: 1575–1580.
6 Perotin JM, Dury S, Renois F, *et al.* Detection of multiple viral and bacterial infections in acute exacerbation of chronic obstructive pulmonary disease: a pilot prospective study. *J Med Virol* 2013; 85: 866–873.
7 Esposito S, Dacco V, Daleno C, *et al.* Human rhinovirus infection in children with cystic fibrosis. *Jpn J Infect Dis* 2014; 67: 399–401.
8 Goffard A, Lambert V, Salleron J, *et al.* Virus and cystic fibrosis: rhinoviruses are associated with exacerbations in adult patients. *J Clin Virol* 2014; 60: 147–153.
9 Kapur N, Mackay IM, Sloots TP, *et al.* Respiratory viruses in exacerbations of non-cystic fibrosis bronchiectasis in children. *Arch Dis Child* 2014; 99: 749–753.
10 Meijer M, Rijkers GT, van Overveld FJ. Neutrophils and emerging targets for treatment in chronic obstructive pulmonary disease. *Expert Rev Clin Immunol* 2013; 9: 1055–1068.
11 Zhu J, Message SD, Qiu Y, *et al.* Airway inflammation and illness severity in response to experimental rhinovirus infection in asthma. *Chest* 2014; 145: 1219–1229.
12 Wang M, Gao P, Wu X, *et al.* Impaired anti-inflammatory action of glucocorticoid in neutrophil from patients with steroid-resistant asthma. *Respir Res* 2016; 17: 153.
13 Singanayagam A, Glanville N, Girkin JL, *et al.* Corticosteroid suppression of antiviral immunity increases bacterial loads and mucus production in COPD exacerbations. *Nat Commun* 2018; 9: 2229.
14 Boehme KW, Compton T. Innate sensing of viruses by toll-like receptors. *J Virol* 2004; 78: 7867–7873.
15 Teijaro JR, Walsh KB, Rice S, *et al.* Mapping the innate signaling cascade essential for cytokine storm during influenza virus infection. *Proc Natl Acad Sci U S A* 2014; 111: 3799–3804.
16 Shah M, Anwar MA, Kim JH, *et al.* Advances in antiviral therapies targeting toll-like receptors. *Expert Opin Investig Drugs* 2016; 25: 437–453.
17 Qiu Y, Pu A, Zheng H, *et al.* TLR2-dependent signaling for IL-15 production is essential for the homeostasis of intestinal intraepithelial lymphocytes. *Mediators Inflamm* 2016; 2016: 4281865.
18 Tan AC, Mifsud EJ, Zeng W, *et al.* Intranasal administration of the TLR2 agonist Pam2Cys provides rapid protection against influenza in mice. *Mol Pharm* 2012; 9: 2710–2718.
19 Wijayadikusumah AR, Sullivan LC, Jackson DC, *et al.* Structure-function relationships of protein-lipopeptide complexes and influence on immunogenicity. *Amino Acids* 2017; 49: 1691–1704.
20 Wark PA, Johnston SL, Bucchieri F, *et al.* Asthmatic bronchial epithelial cells have a deficient innate immune response to infection with rhinovirus. *J Exp Med* 2005; 201: 937–947.
21 Contoli M, Message SD, Laza-Stanca V, *et al.* Role of deficient type III interferon-lambda production in asthma exacerbations. *Nat Med* 2006; 12: 1023–1026.
22 Edwards MR, Regamey N, Vareille M, *et al.* Impaired innate interferon induction in severe therapy resistant atopic asthmatic children. *Mucosal Immunol* 2013; 6: 797–806.
23 Bartlett NW, Walton RP, Edwards MR, *et al.* Mouse models of rhinovirus-induced disease and exacerbation of allergic airway inflammation. *Nat Med* 2008; 14: 199–204.
24 Bartlett NW, Singanayagam A, Johnston SL. Mouse models of rhinovirus infection and airways disease. *Methods Mol Biol* 2015; 1221: 181–188.
25 Stewart CE, Torr EE, Mohd Jamili NH, *et al.* Evaluation of differentiated human bronchial epithelial cell culture systems for asthma research. *J Allergy (Cairo)* 2012; 2012: 943982.
26 Hackett T-L, Singhera GK, Shaheen F, *et al.* Intrinsic phenotypic differences of asthmatic epithelium and its inflammatory responses to respiratory syncytial virus and air pollution. *Am J Respir Cell Mol Biol* 2011; 45: 1090–1100.
27 Martinovich KM, Iosifidis T, Buckley AG, *et al.* Conditionally reprogrammed primary airway epithelial cells maintain morphology, lineage and disease specific functional characteristics. *Sci Rep* 2017; 7: 17971.

28 Nguyen DT, de Witte L, Ludlow M, *et al.* The synthetic bacterial lipopeptide Pam3CSK4 modulates respiratory syncytial virus infection independent of TLR activation. *PLoS Pathog* 2010; 6: e1001049.

29 Message SD, Laza-Stanca V, Mallia P, *et al.* Rhinovirus-induced lower respiratory illness is increased in asthma and related to virus load and Th1/2 cytokine and IL-10 production. *Proc Natl Acad Sci U S A* 2008; 105: 13562–13567.

30 Powell D, Milton M, Perry A, *et al.* drpowell/degust 4.1.1. (Version 4.1.1). Zenodo. http://doi.org/10.5281/zenodo.3501067

31 Babicki S, Arndt D, Marcu A, *et al.* Heatmapper: web-enabled heat mapping for all. *Nucleic Acids Res* 2016; 44: W147–W153.

32 Veerati PC, Troy NM, Reid AT, *et al.* Airway epithelial cell immunity is delayed during rhinovirus infection in asthma and COPD. *Front Immunol* 2020; 11: 974.

33 Ritchie AI, Farne HA, Singanayagam A, *et al.* Pathogenesis of viral infection in exacerbations of airway disease. *Ann Am Thorac Soc* 2015; 12: Suppl. 2, S115–S132.

34 Contoli M, Pauletti A, Rossi MR, *et al.* Long-term effects of inhaled corticosteroids on sputum bacterial and viral loads in COPD. *Eur Respir J* 2017; 50: 1700451.

35 Singanayagam A, Glanville N, Bartlett N, *et al.* Effect of fluticasone propionate on virus-induced airways inflammation and anti-viral immune responses in mice. *Lancet* 2015; 385: Suppl. 1, S88.

36 Gebhardt T, Wakim LM, Eidsmo L, *et al.* Memory T cells in nonlymphoid tissue that provide enhanced local immunity during infection with herpes simplex virus. *Nat Immunol* 2009; 10: 524–530.

37 Watanabe N, Gavrieli M, Sedy JR, *et al.* BTLA is a lymphocyte inhibitory receptor with similarities to CTLA-4 and PD-1. *Nat Immunol* 2003; 4: 670–679.

38 Richter G, Burdach S. ICOS: a new costimulatory ligand/receptor pair and its role in T-cell activion. *Onkologie* 2004; 27: 91–95.

39 Mifsud EJ, Tan ACL, Reading PC, *et al.* Mapping the pulmonary environment of animals protected from virulent H1N1 influenza infection using the TLR-2 agonist Pam2Cys. *Immunol Cell Biol* 2016; 94: 169–176.

40 Blackwell TS, Christman JW. The role of nuclear factor-kappa B in cytokine gene regulation. *Am J Respir Cell Mol Biol* 1997; 17: 3–9.

41 Vogel CF, Wu D, Goth SR, *et al.* Aryl hydrocarbon receptor signaling regulates NF-kappaB RelB activation during dendritic-cell differentiation. *Immunol Cell Biol* 2013; 91: 568–575.

42 Marko L, Vigolo E, Hinze C, *et al.* Tubular epithelial NF-kappaB activity regulates ischemic AKI. *J Am Soc Nephrol* 2016; 27: 2658–2669.

43 Bentley JK, Han M, Jaipalli S, *et al.* Myristoylated rhinovirus VP4 protein activates TLR2-dependent proinflammatory gene expression. *Am J Physiol Lung Cell Mol Physiol* 2019; 317: L57–L70.

44 Pauligk C, Nain M, Reiling N, *et al.* CD14 is required for influenza A virus-induced cytokine and chemokine production. *Immunobiology* 2004; 209: 3–10.

45 Haeberle HA, Takizawa R, Casola A, *et al.* Respiratory syncytial virus-induced activation of nuclear factor-kappaB in the lung involves alveolar macrophages and toll-like receptor 4-dependent pathways. *J Infect Dis* 2002; 186: 1199–1206.

46 Shinya K, Ito M, Makino A, *et al.* The TLR4-TRIF pathway protects against H5N1 influenza virus infection. *J Virol* 2012; 86: 19–24.

47 Khanolkar A, Hartwig SM, Haag BA, *et al.* Toll-like receptor 4 deficiency increases disease and mortality after mouse hepatitis virus type 1 infection of susceptible C3H mice. *J Virol* 2009; 83: 8946–8956.

48 Odendall C, Voak AA, Kagan JC. Type III IFNs are commonly induced by bacteria-Sensing TLRs and reinforce epithelial barriers during infection. *J Immunol* 2017; 199: 3270–3279.

49 Galani IE, Triantafyllia V, Eleminiadou EE, *et al.* Interferon-lambda mediates non-redundant front-line antiviral protection against influenza virus infection without compromising host fitness. *Immunity* 2017; 46: 875–890. e876.